

High-performance organic field-effect transistors with dielectric and active layers printed sequentially by ultrasonic spraying†

Cite this: *J. Mater. Chem. C*, 2013, **1**, 4384

Ming Shao,^{‡a} Sanjib Das,^{‡b} Kai Xiao,^{*a} Jihua Chen,^a Jong K. Keum,^{ac} Ilia N. Ivanov,^a Gong Gu,^b William Durant,^d Dawen Li^d and David B. Geohegan^a

High-performance organic field-effect transistors (OFETs) are reported with dielectric and active layers sequentially deposited by ultrasonic spray-printing. A cross-linkable insulator and a soluble small molecule semiconductor are developed which are both printable and highly robust. Using plastic with pre-patterned indium tin oxide gate contacts as required for display applications, two different layers are sequentially spray-printed: the semiconductor 6,13-bis(trisopropylsilylethynyl)pentacene (TIPS-PEN), and the insulator poly-4-vinylphenol (PVP). OFETs printed in ambient air with a bottom-gate/top-contact geometry are shown to achieve on/off ratios of $>10^4$ and mobilities up to $0.35 \text{ cm}^2 \text{ V}^{-1} \text{ s}^{-1}$. These rival the characteristics of the best solution-processable small molecule FETs fabricated by other processing methods such as drop casting and ink-jet printing.

Received 21st March 2013
Accepted 9th May 2013

DOI: 10.1039/c3tc30535j

www.rsc.org/MaterialsC

1 Introduction

Recent progress in the design and synthesis of organic semiconductor materials have enabled organic field-effect transistors (OFETs) to achieve high charge carrier mobilities comparable to or exceeding that of amorphous silicon.^{1–3} As a result, they have been successfully integrated to enable a wide range of applications including display backplanes, electronic papers, sensors, memories, and radio-frequency (RF) identification tags.^{4–6} However, the lack of low-cost and large-scale OFET manufacturing methods remains a major obstacle to their successful commercialization. To this end, solution processing of organic semiconductors for OFETs is attracting tremendous interest because it is suitable for large area processing, is compatible with flexible substrates, and has the potential to take advantage of existing low-cost, high-throughput, roll-to-roll (R2R) manufacturing technology. Spin-coating and drop-casting are two widely employed solution processing techniques that are simple and effective for producing devices with excellent performance in the research

laboratory environment.^{7,8} However, these techniques are inherently inefficient, wasting high fractions of solution, and are not readily scalable to industrial scale large area processing. Intense efforts have been directed toward the development of alternative solution-based methods such as ink-jet printing, screen printing, doctor blading, and spray coating that can meet the manufacturing requirements for cost-effective, large area processing.^{9–11}

In particular, spray coating is emerging as one of the most promising cost-effective coating techniques for both organic and inorganic films due to its high production speed, efficient use of materials, good reproducibility, and compatibility with different substrates.^{12,13} Several spray technologies have recently been explored for their suitability to deposit functional organic semiconductors in thin films for large area organic electronic devices.^{9,14,15} For example, air-brush spray methods are inexpensive and allow high throughput, but with limited deposition control precision. Nevertheless, a power-conversion efficiency of 2.83% has been reported for a spray-deposited organic photovoltaic (OPV) device by an inexpensive handheld airbrush technique.¹⁶ Evaporative spray deposition from polymer solutions has also shown promise for polymer light-emitting diodes (LEDs) and FET devices, but the required heating of the solution is found to induce undesirably rough surfaces.^{12,17} Ultrasonic spray-coating is a relatively new variant of conventional spray approaches. It has many advantages including picoliter drop sizes, directional spray control *via* deflection with an inert gas, large-area uniform coverage for thin films, and the potential for the deposition of continuous layers.¹⁸ The key advantage of the technique is the use of supersmall droplets that minimize the dissolution of any underlying layers.¹⁹ A narrow distribution of

^aCenter for Nanophase Materials Sciences, Oak Ridge National Laboratory, One Bethel Valley Road, Oak Ridge, TN, 37831, USA. E-mail: xiaok@ornl.gov

^bDepartment of Electrical Engineering and Computer Sciences, University of Tennessee at Knoxville, Knoxville, TN, 37931, USA

^cNeutron Scattering Science Division, Oak Ridge National Laboratory, One Bethel Valley Road, Oak Ridge, TN, 37831, USA

^dDepartment of Electrical and Computer Engineering, University of Alabama, Tuscaloosa, AL 35487, USA

† Electronic supplementary information (ESI) available. See DOI: 10.1039/c3tc30535j

‡ These authors (M. S. and S. D.) contributed equally.

tiny droplets land on the surface to produce, in the case of large flow rates, a thin yet continuous wet layer, or in the case of reduced flow rates, depositions characterized by sparse arrangements of dots that dry independently. Although ultrasonic spray-coating has been demonstrated as an alternative method to fabricate organic electronic devices including OLEDs,^{20,21} OPVs,^{18,19,22} and organic photodetectors (OPDs),²³ very little work concerning OFET fabrication by this process has been reported.²⁴ Previous work has mostly focused on the spray coating of soluble conjugated polymers such as poly(3-hexylthiophene) (P3HT).^{19,24} Compared to polymers, however, soluble small molecules are easier to synthesize and purify, and exhibit better charge carrier mobility and chemical stability.²⁵

A typical, soluble small molecule organic semiconductor that is widely used in organic electronics because of its high mobility and good air stability is 6,13-bis(triisopropylsilylethynyl)pentacene (TIPS-PEN).²⁶ So far, high mobility TIPS-PEN based OFETs have been fabricated by a variety of solution-based methods including spin-coating and drop-casting. TIPS-PEN OFETs prepared by drop-casting have exhibited high mobilities of $0.65 \text{ cm}^2 \text{ V}^{-1} \text{ s}^{-1}$ while those prepared by spin-coating usually show relatively lower mobilities, ranging between 0.05 and $0.20 \text{ cm}^2 \text{ V}^{-1} \text{ s}^{-1}$.²⁷ Ink-jet printing of TIPS-PEN OFETs with mobilities of $0.12 \text{ cm}^2 \text{ V}^{-1} \text{ s}^{-1}$ have also been reported.²⁸ To our knowledge, so far there have been no reports of TIPS-PEN OFETs prepared by the ultrasonic spray technique, a process that is compatible for the fabrication of large area, cost-effective OFETs.

In this work, a fabrication method for high-performance OFETs was developed based on ultrasonic spray-coated TIPS-PEN active layers, as well as spray-coated poly-4-vinylphenol (PVP) dielectric layers on various substrates. Highly crystalline, aligned TIPS-PEN films were obtained on $\text{SiO}_2\text{-n}^{++}$ Si substrate by optimizing ultrasonic spray parameters such as flow-rate,

nozzle height and moving speed, resulting in a maximum mobility as high as $0.36 \text{ cm}^2 \text{ V}^{-1} \text{ s}^{-1}$ and an on/off current ratio greater than 10^5 . Moreover, flexible OFETs were fabricated by the sequential spray deposition of a dielectric layer of PVP and an active layer of TIPS-PEN on poly(ethylene terephthalate) (PET) plastic substrates. The flexible TIPS-PEN OFETs exhibit the best mobility up to $0.35 \text{ cm}^2 \text{ V}^{-1} \text{ s}^{-1}$ and an on/off ratio of more than 10^4 , together with negligible hysteresis in current-voltage characteristics. Ultrasonic spray-coating of OFETs thus provides a device performance comparable or superior to similar devices prepared by other solution processing methods. As a result, ultrasonic spray-coating is a promising, cost-effective method for large-area integrated flexible electronics applications.

2 Results and discussion

Fig. 1(a) shows a schematic illustration of the ultrasonic spray-coating process and the structure of fabricated bottom gate/top contact (BG/TC) OFET devices. For the rigid $\text{SiO}_2\text{-n}^{++}$ Si substrate, the TIPS-PEN solution was first deposited *via* ultrasonic spray-coating and then Au source-drain electrodes were deposited on the oriented TIPS-PEN crystalline film. Fig. 1(b) shows a polarized optical microscopy image of the top view of the TIPS-PEN film sprayed from a 0.8 wt% toluene solution. As the solvent evaporation proceeds, long, ribbon-shaped TIPS-PEN polycrystals containing some single-crystalline domains were observed to grow as indicated by their color variation under polarized light. The typical TIPS-PEN crystals observed in the spray-coated films were several hundred micrometers long and tens of micrometers wide. In general, the charge transport in polycrystalline TIPS-PEN films is quite different in the two types of regions: the high-mobility large crystalline grains and

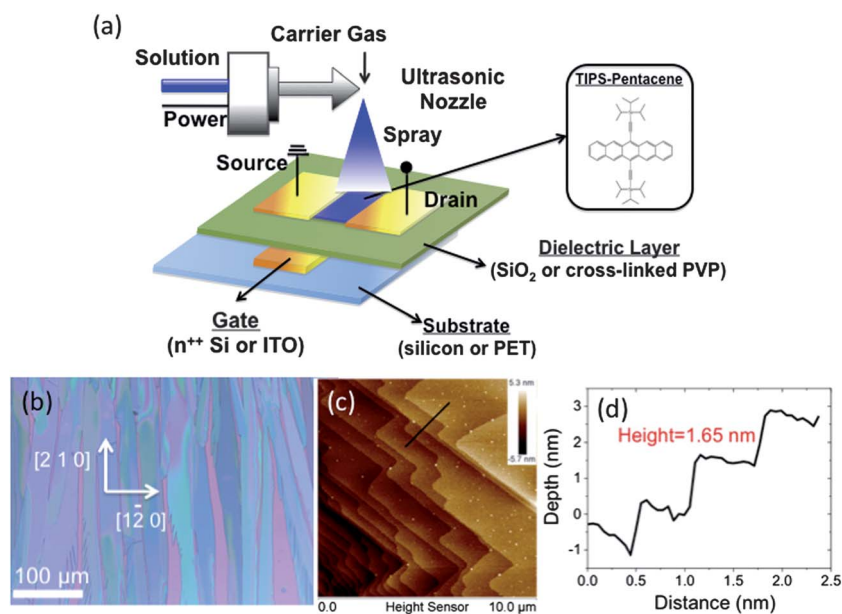


Fig. 1 (a) Schematic diagram of the ultrasonic spray process and the bottom-gate (BG) top-contact (TC) OFET device architecture. The chemical structure of TIPS-PEN is shown in the inset. In the Si substrate case, the n^{++} doped Si substrate serves as the unpatterned gate. (b) Polarized optical microscopy image of a spray-coated TIPS-PEN film, (c) AFM image of a terraced structure for a sprayed TIPS-PEN film, (d) line profile taken along the black line segment in (c) crossing three single steps.

the low-mobility polycrystalline regions with many grain boundaries. The large-grained, ribbon-shaped TIPS-PEN polycrystals appear to be responsible for the higher field-effect mobilities because the charge carriers encounter fewer grain boundaries in these regions. Fig. 1(c) shows an atomic force microscopy (AFM) image of a sprayed TIPS-PEN film. The well-developed terrace-like multilayered structure indicates the formation of a highly crystalline film. The mean step height per terrace measured from the cross-sectional AFM profile in Fig. 1(d) is around 1.65 nm, which is in agreement with the vertical intermolecular spacing in TIPS-PEN single crystals.^{26,29} This result suggests that the TIPS-PEN in the sprayed film is oriented in a (001) orientation with the pentacene backbone packed in a face-to-face orientation.

The molecule orientation and packing in the spray-coated TIPS-PEN films were further confirmed by out-of-plane X-ray diffraction (XRD) and two-dimensional (2D) grazing-incident X-ray diffraction (GIXD) studies. Fig. 2(a) shows the out-of-plane XRD patterns of a sprayed TIPS-PEN film, which consists only of a series of (00*l*) reflection diffraction peaks, indicating a well-organized molecular crystal structure with a vertical intermolecular spacing of 1.68 nm. This result is consistent with the terrace step height of 16–17 Å measured from AFM images, which is identical to that of the *c*-axis unit cell.³⁰ Fig. 2(b) shows an in-plane GIXD pattern of a spray-coated TIPS-PEN film on SiO₂, exhibiting many scattering spots along the *Q_z* and the *Q_{x,y}* directions. The (01*l*) diffraction peaks, corresponding to the repeating period perpendicular to the direction of crystal growth, and (00*l*) diffraction peaks, corresponding to the repeating period parallel to the direction of crystal growth, were observed, indicating that the crystals are azimuthally oriented. These results demonstrated that well-ordered TIPS-PEN crystals in the lateral and vertical directions are formed in the ultrasonic spray-coating process.

Fig. 3 shows the typical transfer and output curves of OFETs based on TIPS-PEN sprayed on SiO₂-n⁺ Si substrates. The average mobility of 20 sprayed devices is 0.15 ± 0.02 cm² V⁻¹ s⁻¹, with a maximum of 0.36 cm² V⁻¹ s⁻¹. The average threshold voltage is -0.9 ± 3.8 V and the on/off current ratio is 1.3 × 10⁵. Negligible current hysteresis was observed in the transfer characteristics, indicating few charge trapping centers between the polycrystalline surface of TIPS-PEN and the gate dielectric layer. The uniformity of the electrical properties was examined

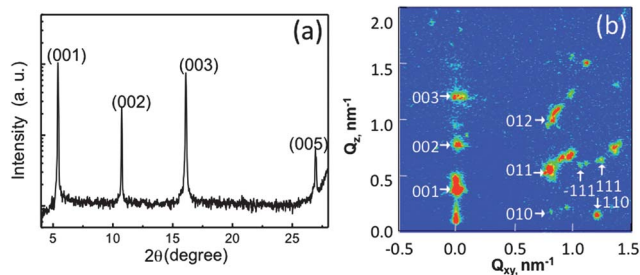


Fig. 2 (a) Out-of-plane X-ray diffraction pattern, and (b) 2D GIXD image of a spray-coated TIPS-PEN film on SiO₂. Indices are provided for the most intense Bragg rods.

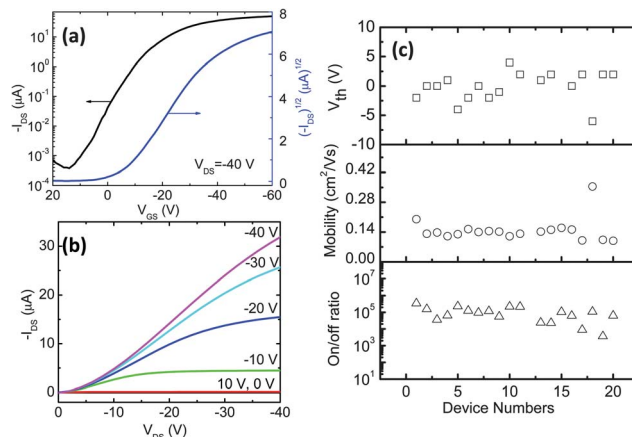


Fig. 3 (a) Representative transfer (at a drain bias of -40 V) and (b) output characteristics of a spray-coated TIPS-PEN OFET on a SiO₂-Si substrate with a channel width of 2000 μm and channel length of 100 μm. (c) Variation of device performance parameters including mobility, threshold voltage, and on/off ratio for 20 devices.

by selecting 20 transistor devices. The variations in the values of the characteristic parameters of these devices are shown in Fig. 3(c). The mobility, threshold voltage (*V_{th}*), and on/off ratio fluctuate slightly, but overall, the electrical properties were found to be uniform. These results suggest that the spray-coating method can be used to fabricate a variety of printed electronic devices that exhibit a high degree of inter-device uniformity. The performance of the spray-coated devices is comparable to that of TIPS-PEN OFETs fabricated by a drop-casting process and better than those of devices fabricated by spin-coating process, as shown in Table 1.

The boiling point (bp) and vapor pressure of the solvent could change the drying behavior of droplets in a spray process and hence significantly affect the morphology and crystallinity of the spray-coated TIPS-PEN film. Therefore, we fabricated TIPS-PEN OFETs using three solvents, toluene (bp = 111 °C), chlorobenzene (bp = 131 °C) and 1,2-dichlorobenzene (ODCB) (bp = 180 °C) to investigate their suitability for the ultrasonic spray technique. The lower evaporation rate of these high boiling point solvents makes the coating process less sensitive and easier to control over a large parameter space. The device performances of spray-coated TIPS-PEN OFETs with different solvents are compared in Fig. S2.† The mobility is 0.05 cm² V⁻¹ s⁻¹ for films sprayed from a chlorobenzene solution, 0.03 cm² V⁻¹ s⁻¹ for ODCB, and 0.16 cm² V⁻¹ s⁻¹ for toluene. The results show that the highest boiling point solvent does not necessarily provide the highest mobility and suggest toluene with medium boiling point to be the most suitable solvent for the TIPS-PEN deposition by ultrasonic spraying, which is consistent with other literature reports.^{31,32} The performance of OFETs strongly depends on the morphology of TIPS-PEN polycrystal films. TIPS-PEN films with high crystallinity and large grain size exhibit the best mobility and on/off ratio. Particularly, in our ultrasonic spray process, balancing the solvent evaporation and diffusion-driven flows of solution droplets is critical to obtain highly ordered TIPS-PEN crystals. The moderate evaporation rate of

Table 1 Electrical properties of TIPS-PEN FETs with BG/TC device geometry fabricated by different methods. The mobilities were calculated at the saturation region at a drain bias of -40 V^a

Substrate	Insulator		Active layer Processing	μ^{avg} ($\text{cm}^2 \text{V}^{-1} \text{s}^{-1}$)	V_{th} (V)	On/off ratio
	Material	Processing				
Si	SiO ₂	Thermal oxide	Spin-coating	0.0005	-7.6	1×10^3
			Drop-casting	0.157	7.0	8×10^4
			Spray-coating	0.145	-0.9	1×10^5
PET	PVP	Spin-coating	Spray-coating	0.117	2.0	6×10^4
			Spray-coating	0.108	3.6	2×10^4
			Spray-coating	0.100	1.6	4×10^4
			Spray-coating	0.122	11.3	1×10^4

^a Average values were obtained from more than 20 devices.

toluene can improve the morphology uniformity and packing density of the TIPS-PEN molecules, and therefore exhibit the best device performance.³²

In addition, film formation by spray-coating is a complex process that is affected not only by the solvent boiling point but also by other factors such as the infuse rate and nozzle moving speed. The effects of the infuse rate, nozzle-substrate distance, and nozzle moving speed on the performance of the spray-coated devices were also studied. Fig. S3† shows the relationship of device mobility with changing the infuse rate, nozzle-substrate distance, or nozzle moving speed while the other parameters were held constant. From this plot, the optimized processing conditions for spray-coated TIPS-PEN films in this work are determined to be a flow rate of 1.2 ml min^{-1} , nozzle-to-substrate height of 4.6 cm , and nozzle moving speed of 8 mm s^{-1} .

To demonstrate the versatility of the ultrasonic spray technique, we also explored the deposition of a dielectric layer by ultrasonic spraying to fabricate flexible OFETs. A wide range of insulators with different solvents have been used in various deposition techniques for OFETs.^{29,30} In this work, a cross-linkable PVP³³ was selected to improve the environmental stability and structural robustness and to enhance the chemical stability to minimize potential solubility issues arising from subsequently deposited layers. In order to get a smooth film, we focused on a single-pass deposition technique to spray the PVP dielectric layer. During the spray process, the dispersed droplets merged into a single wet surface layer on the substrate before drying. As the solvent evaporates, a uniform PVP film was successfully coated with the additive poly(melamine-*co*-formaldehyde) in propylene glycol monomethyl ether acetate (PGMEA) on the substrate. Pre-heating the substrate up to 50°C can facilitate the merging of droplets, speed up the drying process, and improve the homogeneity of the PVP film (Fig. S4†). The coating was followed by a heating cycle at 175°C for an hour to induce crosslinking. At this temperature, crosslinker poly(melamine-*co*-formaldehyde) efficiently acts as a donor of a formaldehyde moiety by firstly reacting at the activated 3-position of the phenol ring in PVP. Then, the cross-linking process is completed by reacting with another phenol ring to form a strong covalent-bonded bridge. Crosslinked PVP films are not dissolved in common organic solvents such as chloroform,

toluene, or chlorobenzene, allowing for subsequent solution-based deposition of organic semiconductors. Fig. 4(a) shows an optical image of a spray-coated PVP film. A uniform PVP film was obtained over a large area. We also observed some bumps and craters on the film, induced by the impingement of sprayed droplets and convergence on droplet boundaries. A similar phenomenon was reported earlier in other sprayed films.²⁴ The resultant spray-coated PVP insulator layer at optimized spray conditions has a thickness of around 600 nm . The root-mean-square (RMS) roughness of the local spray-printed PVP

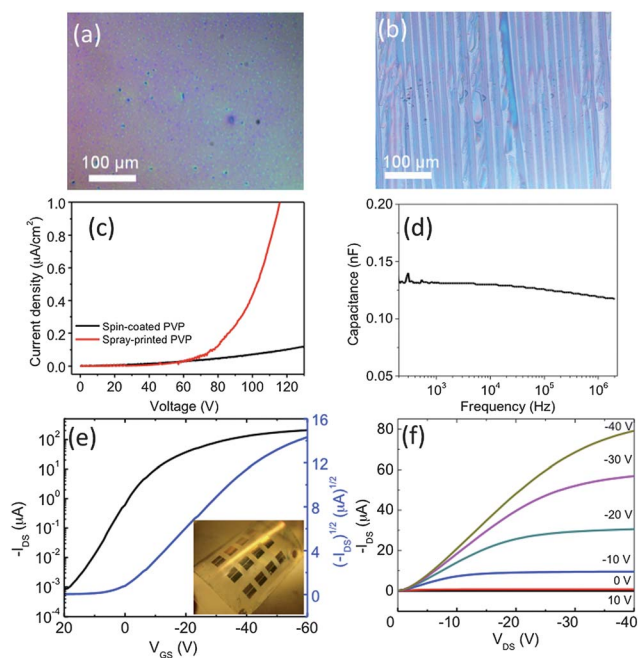


Fig. 4 (a) Optical microscopy image of a spray-coated PVP film prepared at 50°C , (b) optical microscopy image of a sequentially spray-coated TIPS-PEN film on a PVP layer, (c) current leakage versus applied voltage curves of PVA films prepared by ultrasonic spraying and spin-coating processes. The electrical measurements were performed using Si-PVP-Al structures fabricated on highly doped silicon substrates. (d) Frequency-dependent capacitance of the spray-coated PVP film measured up to 1 MHz . (e) Transfer and (f) output characteristics of ultrasonic spray-coated TIPS-PEN based flexible OFETs with sequentially deposited dielectric (PVP) and semiconductor (TIPS-PEN) layers, pictured in the inset of (e).

film is 0.46 nm (across a $5\ \mu\text{m} \times 5\ \mu\text{m}$ area), determined by AFM measurements (Fig. S6†), similar to the roughness of spin-coated films ($\sim 0.30\ \text{nm}$). The low roughness is mainly due to the small size of droplets atomized by ultrasonic waves. The capacitance per unit area was found to be equal to $6.2\ \text{nF cm}^{-2}$. The PVP films exhibit excellent dielectric properties with a large breakdown voltage over 100 V and sufficiently low leakage current densities in the 10^{-7} to $10^{-8}\ \text{A cm}^{-2}$ range at device operating voltages, as shown in Fig. 4(c). The capacitance does not significantly change for wide frequency sweeps (20 Hz–2 MHz) as shown in Fig. 4(d). These results indicate the sprayed PVP films have good film quality and meets the requirements for the dielectric gate of flexible OFETs.

After the formation of the dielectric layer, the TIPS-PEN semiconductor was subsequently sprayed on top of the PVP film. The sprayed TIPS-PEN solution does not dissolve the PVP film and long ribbon-shaped TIPS-PEN polycrystals form on the spray-coated PVP layer, as shown in Fig. 4(b), similar to that observed on the SiO_2 -Si substrate. Devices with spray-coated, cross-linked PVP on a highly doped silicon substrate exhibited an average mobility of $0.11 \pm 0.03\ \text{cm}^2\ \text{V}^{-1}\ \text{s}^{-1}$. This is comparable to the values achieved for devices using spin-coated cross-linked PVP as the insulator layer on a silicon substrate (see Table 1). We also fabricated flexible TIPS-PEN OFETs, which were prepared on PET flexible substrates with patterned ITO electrodes using sequentially spray-coated layers of PVP dielectric and TIPS-PEN semiconductor, as shown in the inset of Fig. 4(e). The spray-coated, flexible OFETs exhibit a maximum mobility of $0.35\ \text{cm}^2\ \text{V}^{-1}\ \text{s}^{-1}$, with an average mobility of $0.12 \pm 0.02\ \text{cm}^2\ \text{V}^{-1}\ \text{s}^{-1}$, a threshold voltage of $11.3 \pm 2.5\ \text{V}$, and an on-off current ratio $>10^4$, as shown in Fig. 4(e) and (f). Device parameters of the TIPS-PEN FET fabricated on rigid and flexible substrate using sequentially spray process are summarized in Table 1. In all cases, the mobilities and on/off ratios are consistent with those obtained in other solution-processing methods. Additionally, a bending test demonstrated no deterioration in the drain current even when the devices were bent to a bending radius as small as 9 mm. No significant changes in the OFET performance after 20 bending cycles were observed except a slight increase in the off current (Fig. S8†), probably due to the polymer dielectric or TIPS-PEN degradation.^{34,35} Therefore, ultrasonic spraying is generally usable for a wide variety of solution-processible polymers and small molecules for flexible, large area organic electronic devices.

3 Conclusions

In summary, we have demonstrated a novel, scalable deposition technique, the ultrasonic spraying process, for coating small molecule semiconductor and polymer insulator films for high-performance OFETs. Aligned, well-organized, ribbon-shaped TIPS-PEN polycrystal films were formed on both rigid and flexible substrates using the ultrasonic spray process. The spray-coated, crosslinked PVP dielectric films have smooth surfaces over a large area along with excellent dielectric properties. Thus, the high-performance, flexible OFETs were fabricated using sequentially spray-coated TIPS-PEN semiconductor and PVP

insulator layers on a plastic substrate at optimized processing parameters, including the choice of solvent, solution infuse rate, nozzle-substrate distance, and nozzle moving speed. The TIPS-PEN OFETs exhibited excellent device performances with a maximum hole mobility of $0.36\ \text{cm}^2\ \text{V}^{-1}\ \text{s}^{-1}$, a low threshold voltage of $-1\ \text{V}$ and on-off current ratio larger than 10^5 , which are comparable or even superior to those obtained with conventional solution processing methods such as drop-casting and spin-coating. Our experimental results successfully demonstrated that ultrasonic spraying is a promising cost-effective, scalable method to fabricate large-area and flexible OFETs for industrial production.

4 Experimental section

4.1 Materials and spray solution

The poly(4-vinylphenol) (PVP, $M_w = 20\ \text{kDa}$) and a cross-linking agent poly(melamine-co-formaldehyde) ($M_w = 432$) were purchased from Sigma Aldrich. A 1.5 wt% PVP solution was first prepared with propylene glycol monomethyl ether acetate (PGMEA) as the solvent. Then, the poly(melamine-co-formaldehyde) was added to the solution at a weight ratio of 1 : 3 to PVP. The blend solution was stirred using a magnetic spin bar at room temperature for 24 h. 6,13-Bis(triisopropylsilyl)ethynyl pentacene (TIPS-PEN) was used as purchased from Sigma Aldrich without further purification. TIPS-PEN was dissolved in toluene at a concentration of $8\ \text{mg ml}^{-1}$.

4.2 Layer preparation

Ultrasonic spraying was performed under ambient conditions with an ExactoCoat system from Sono-Tek Corporation equipped with a 120 kHz ultrasonic atomizing nozzle. The spray system can support a substrate of up to $200 \times 200\ \text{mm}^2$. The ultrasonic spray deposition system used in this study is shown schematically in Fig. 1. The ink solution was fed by a calibrated computer controlled syringe pump dispersion system. The ultrasonic nozzle atomizes the ink solution into micrometer size droplets with a high surface to mass ratio. In addition, the ultrasound prevents ink clogging in the nozzle head over a wide range of solution concentrations. The atomized solution is directed onto a substrate by an argon carrier gas. Computer control allows reproducible depositions with precise deposition rates. The substrate is tilted at a small angle (3°) to align the orientation of the TIPS-PEN crystals while the solution is sprayed on the substrate. In all our experiments the atomizing gas pressure for the spray process was kept at 0.4 psi in order to achieve a reasonable spray rate. Spray-coated films are optimized by varying the solution flow rate, nozzle movement speed, spray nozzle height and substrate temperature. The optimized processing conditions for TIPS-PEN film in this work are: a flow rate of $1.2\ \text{ml min}^{-1}$, nozzle-to-substrate height of 4.6 cm, and nozzle moving speed of $8\ \text{mm s}^{-1}$.

4.3 Spin-coated and drop-cast OFETs

The same $8\ \text{mg ml}^{-1}$ TIPS-PEN solution in toluene was spin-coated (500 rpm and 60 s) or drop-cast onto the SiO_2 -Si

substrate and the device structures were prepared using the same method as used for the spray-coated OFETs.

4.4 Characterization

Optical micrographs of thin films were collected using a Nikon OptiPhot2-POL optical microscope with cross-polarizers. Thin film crystallinity was characterized using Philips X'Pert X-ray diffraction. 2D GIXD data were collected as a 2D image map using an image plate that was divided into a component in the plane of the substrate and a component perpendicular to the substrate in an Anton Paar SAXSess mc2 spectrometer (high-resolution grazing incidence scattering with a point X-ray beam). Morphology and roughness of sprayed films were investigated using a Bruker Dimension Icon Atomic Force Microscope (AFM) operated in a tapping mode.

4.5 Device fabrication and testing

A bottom-gate, top-contact configuration as shown in Fig. 1 was adopted for the OFET fabrication. Prior to the spray deposition of organic thin films, heavily doped n-type silicon substrates with 300 nm thermally grown silicon dioxide (capacitance, $C_i = 12.5 \text{ nF cm}^{-2}$), and ITO coated PET substrates were cleaned with a sequence of detergent, DI water, acetone and isopropyl alcohol (IPA) in an ultrasonic bath. The PVP solution was ultrasonic spray-coated on the pre-cleaned ITO coated polyethylene terephthalate (PET) flexible substrates. Then, the sprayed PVP films were cross-linked at 180°C for 1 h. After the crosslinking of the PVP dielectric layer, the TIPS-PEN was subsequently spray-coated on top of the PVP film. For devices using the Si substrate, TIPS-PEN was directly sprayed onto the SiO_2 surface. Since both TIP-PEN and PVP are air stable, all the films were ultrasonically spray-coated under ambient conditions. Finally, a 50 nm thick Au source and drain electrodes were deposited by thermal evaporation through a shadow mask. Channel lengths included 25, 50, 75 and 100 μm , while the width was fixed at 2000 μm . In order to compare the OFET devices fabricated by spray processing, spin-coated and drop-casted OFETs were fabricated. Electrical measurements of OFETs are carried out under ambient conditions with a Keithley 4200 semiconductor analyzer attached to a probe station. By exploiting the slope of transfer curve ($I_{\text{DS}}^{1/2} - V_{\text{GS}}$), the field-effect mobility in the saturation regime is calculated from the equation $I_{\text{DS}} = \mu WC_i (V_{\text{GS}} - V_{\text{T}})^2 / 2L$, where W and L are the channel width and length, C_i is the capacitance per unit area, μ is the field-effect mobility, and V_{GS} and V_{T} are gate voltage and threshold voltage, respectively. The capacitance of the dielectric layer was measured with an Agilent E4980A precision LCR meter.

Acknowledgements

This research was conducted at the Center for Nanophase Materials Sciences (CNMS), which is sponsored at Oak Ridge National Laboratory by the Division of Scientific User Facilities, U.S. Department of Energy, managed by UT-Battelle, LLC, for the U.S. Department of Energy. K.X. and W.D. acknowledge

support from the Higher Education Research Experiences (HERE) summer intern program at ORNL, and D.L. acknowledges partial support from DOE travel fund (08-0217).

References

- H. Yan, Z. H. Chen, Y. Zheng, C. Newman, J. R. Quinn, F. Dotz, M. Kastler and A. Facchetti, *Nature*, 2009, **457**, 679–686.
- H. N. Tsao, D. M. Cho, I. Park, M. R. Hansen, A. Mavrinskiy, D. Y. Yoon, R. Graf, W. Pisula, H. W. Spiess and K. Mullen, *J. Am. Chem. Soc.*, 2011, **133**, 2605–2612.
- H. Minemawari, T. Yamada, H. Matsui, J. Tsutsumi, S. Haas, R. Chiba, R. Kumai and T. Hasegawa, *Nature*, 2011, **475**, 364–367.
- G. H. Gelinck, H. E. A. Huitema, E. Van Veenendaal, E. Cantatore, L. Schrijnemakers, J. B. P. H. Van der Putten, T. C. T. Geuns, M. Beenhakkers, J. B. Giesbers, B. H. Huisman, E. J. Meijer, E. M. Benito, F. J. Touwslager, A. W. Marsman, B. J. E. Van Rens and D. M. De Leeuw, *Nat. Mater.*, 2004, **3**, 106–110.
- T. Sekitani, T. Yokota, U. Zschieschang, H. Klauk, S. Bauer, K. Takeuchi, M. Takamiya, T. Sakurai and T. Someya, *Science*, 2009, **326**, 1516–1519.
- L. Li, L. Jiang, W. Wang, C. Du, H. Fuchs, W. Hu and L. Chi, *Adv. Mater.*, 2012, **24**, 2159–2164.
- J. Li, Y. Zhao, H. S. Tan, Y. L. Guo, C. A. Di, G. Yu, Y. Q. Liu, M. Lin, S. H. Lim, Y. H. Zhou, H. B. Su and B. S. Ong, *Sci. Rep.*, 2012, **2**, 754.
- A. Lv, S. R. Puniredd, J. Zhang, Z. Li, H. Zhu, W. Jiang, H. Dong, Y. He, L. Jiang, Y. Li, W. Pisula, W. Hu and Z. Wang, *Adv. Mater.*, 2012, **24**, 2626–2630.
- P. F. Moonen, I. Yakimets and J. Huskens, *Adv. Mater.*, 2012, **24**, 5526–5541.
- N. Stutzmann, R. H. Friend and H. Sirringhaus, *Science*, 2003, **299**, 1881–1884.
- G. Giri, E. Verploegen, S. C. B. Mannsfeld, S. Atahan-Evrenk, D. H. Kim, S. Y. Lee, H. A. Becerril, A. Aspuru-Guzik, M. F. Toney and Z. Bao, *Nature*, 2011, **480**, 504–508.
- T. Ishikawa, M. Nakamura, K. Fujita and T. Tsutsui, *Appl. Phys. Lett.*, 2004, **84**, 2424–2426.
- M. Lefort, G. Popa, E. Seyrek, R. Szamocki, O. Felix, J. Hemmerle, L. Vidal, J. C. Voegel, F. Boulmedais, G. Decher and P. Schaaf, *Angew. Chem., Int. Ed.*, 2010, **49**, 10110–10113.
- C. K. Chan, L. J. Richter, B. Dinardo, C. Jaye, B. R. Conrad, H. W. Ro, D. S. Germack, D. A. Fischer, D. M. DeLongchamp and D. J. Gundlach, *Appl. Phys. Lett.*, 2010, **96**, 133304.
- S. I. Na, B. K. Yu, S. S. Kim, D. Vak, T. S. Kim, J. S. Yeo and D. Y. Kim, *Sol. Energy Mater. Sol. Cells*, 2010, **94**, 1333–1337.
- L. M. Chen, Z. R. Hong, W. L. Kwan, C. H. Lu, Y. F. Lai, B. Lei, C. P. Liu and Y. Yang, *ACS Nano*, 2010, **4**, 4744–4752.
- Y. Aoki, M. Shakutsui and K. Fujita, *Thin Solid Films*, 2009, **518**, 493–496.

- 18 R. C. Tenent, T. M. Barnes, J. D. Bergeson, A. J. Ferguson, B. To, L. M. Gedvilas, M. J. Heben and J. L. Blackburn, *Adv. Mater.*, 2009, **21**, 3210–3216.
- 19 C. Girotto, D. Moia, B. P. Rand and P. Heremans, *Adv. Funct. Mater.*, 2011, **21**, 64–72.
- 20 T. L. Breen, P. M. Fryer, R. W. Nunes and M. E. Rothwell, *Langmuir*, 2002, **18**, 194–197.
- 21 J. Ju, Y. Yamagata and T. Higuchi, *Adv. Mater.*, 2009, **21**, 4343–4347.
- 22 K. X. Steirer, M. O. Reese, B. L. Rupert, N. Kopidakis, D. C. Olson, R. T. Collins and D. S. Ginley, *Sol. Energy Mater. Sol. Cells*, 2009, **93**, 447–453.
- 23 S. F. Tedde, J. Kern, T. Sterzl, J. Furst, P. Lugli and O. Hayden, *Nano Lett.*, 2009, **9**, 980–983.
- 24 A. Abdellah, B. Fabel, P. Lugli and G. Scarpa, *Org. Electron.*, 2010, **11**, 1031–1038.
- 25 K. Xiao, Y. Liu, T. Qi, W. Zhang, F. Wang, J. Gao, W. Qiu, Y. Ma, G. Cui, S. Chen, X. Zhan, G. Yu, J. Qin, W. Hu and D. Zhu, *J. Am. Chem. Soc.*, 2005, **127**, 13281–13286.
- 26 J. E. Anthony, *Chem. Rev.*, 2006, **106**, 5028–5048.
- 27 S. K. Park, T. N. Jackson, J. E. Anthony and D. A. Mourey, *Appl. Phys. Lett.*, 2007, **91**, 063514.
- 28 J. A. Lim, W. H. Lee, H. S. Lee, J. H. Lee, Y. D. Park and K. Cho, *Adv. Funct. Mater.*, 2008, **18**, 229–234.
- 29 S. C. B. Mannsfeld, M. L. Tang and Z. A. Bao, *Adv. Mater.*, 2011, **23**, 127–131.
- 30 J. H. Chen, C. K. Tee, M. Shtein, J. Anthony and D. C. Martin, *J. Appl. Phys.*, 2008, **103**, 114513.
- 31 C. S. Kim, S. Lee, E. D. Gomez, J. E. Anthony and Y. L. Loo, *Appl. Phys. Lett.*, 2008, **93**, 103302.
- 32 K. Lee, J. Kim, K. Shin and Y. S. Kim, *J. Mater. Chem.*, 2012, **22**, 22763.
- 33 M. Halik, H. Klauk, U. Zschieschang, G. Schmid, W. Radlik and W. Weber, *Adv. Mater.*, 2002, **14**, 1717–1722.
- 34 H. Y. Noh, Y. G. Seol and N. E. Lee, *Appl. Phys. Lett.*, 2009, **95**, 113302.
- 35 T. Sekitani, V. Zschieschang, H. Klauk and T. Someya, *Nat. Mater.*, 2010, **9**, 1015–1022.